www.ethanpublishing.com

International Journal of Mechanical Engineering and Automation

Volume 1, Number 1, July 2014

Contents

Int. J. Mech. Eng. Autom.
Volume 1, Number 1, 2014, pp. 1-10
Received: May 6, 2014; Published: July 25, 2014

International Journal of
Mechanical Engineering
and Automation

A Methodology for Modeling Stress Corrosion Cracking with an Example

Omar Fernandes Aly[1], Miguel Mattar Neto[1] and Mônica Maria de Abreu Mendonça Schvartzman[2]

1. IPEN-Energy and Nuclear Research Institute, São Paulo University, São Paulo, SP 05508-000, Brazil

2. CDTN-Nuclear Technology Development Center, Federal University of Minas Gerais, Belo Horizonte, MG 31270-901, Brazil

Abstract: Stress corrosion cracking is a severe life degradation mode, in nuclear and other industries components (such as pressure vessels, its accessories, piping). It can produce serious accidents, which can put on risk the safety, reliability, and efficiency of those. These failures are of complex prediction, due to many parameters, on which this cracking process depends, such as micro-structural type (grain boundary microchemistry, thermal treatments, grain size, cold work and plastic deformation), mechanical (residual stress, applied stress, strain and strain rate), and environmental (temperature, pH, environment chemical composition, hydrogen partial pressure, electrochemical potential). These parameters determine the thermodynamic conditions which are necessary to initiate and to grow cracking, through the dissolution rate proportional to anodic current density combined with the mechanical action of stress and strain. One presents in this paper a methodology for modeling the stress corrosion cracking, which consists in: data collecting for material testing; determination of corrosion mode of stress corrosion thermodynamic propensity which can be done over a potential vs. pH diagram considering the material and environment; superimposition of an adequate initiation and growing model to describe the process kinetics; these kinetic models can be chose in some of the main applicable for the case study—components (control rod displacement nozzles) made and welded with nickel alloys (alloys 600, 182, and 82) from PWR (pressurized water reactor) nuclear reactor's pressure vessels. The environment is primary water at high temperature (about 300 °C); preliminary results are shown departing of experimental data from slow strain rate test; discussion, conclusion and recommendations.

Key words: Fracture mechanics, light water reactors, models, nickel alloys, stress corrosion.

1. Introduction

The SCC (stress corrosion cracking) initiation and propagation are very complex processes, one modality of EAC (environmentally assisted cracking), besides corrosion fatigue and hydrogen embrittlement, depending on several parameters which can be classified in microstructural, mechanical and environmental [1, 2].

The microstructural factors are [3]: (1) grain boundary chemistry and segregation; (2) thermal treatment which can causes intragranular and intergranular metallic carbide distribution; (3) grain size and cold work or plastic deformation—the two last ones fix the yield strength: these factors can be described as A in Fig. 1 [4]. The mechanical factors are (4) applied and residual stresses: these stresses and geometry can be summarized as stress intensity K (optionally, strain and strain rate which can be also described related to stresses). The environmental factors include: (5) temperature T; (6) activity of $[H]^+$ or pH; (7) solution or water chemistry; (8) inhibitors or pollutants in solution: these two last ones can be described as $[x]$ in Fig. 1; (9) electrode and corrosion potentials E and E_o; (10) partial pressure of hydrogen which reflects on potential. This environmental cracking susceptibility can be expressed as showed in Fig. 1.

For stainless steel and nickel alloys in boiler and

Corresponding author: Omar Fernandes Aly, D.Sc., mechanical engineer, researcher, research field: stress corrosion. E-mail: ofaly@ipen.br; ofaly1@gmail.com.

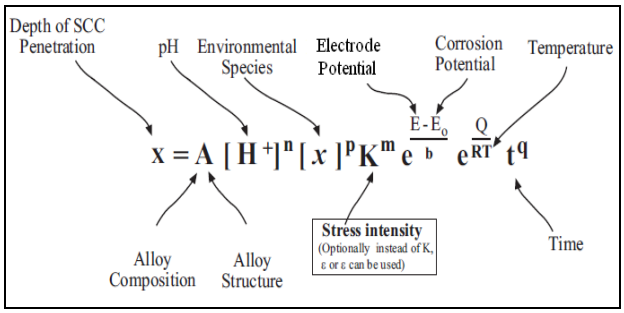

Fig. 1 General phenomenological relationship for SCC process depending on many parameters [4].

primary water at high temperature, there are several mechanisms which allow to express mathematically the stress corrosion cracking initiation and propagation kinetic processes: the Rice's creep model, the creep model derived from Monkman-Grant correlation [5], the slip-step dissolution and film rupture model of Ford and Andresen [6], the internal oxidation mechanism of Scott and Le Calvar [7], the coupled environment fracture model of Macdonald and Urquidi-Macdonald, the enhanced surface mobility theory of Galvele, the numerical model of Rebak and Smialowska, hydrogen induced cracking models of Shen and Shewmon, Magnin and others [3], semi-empirical models of Staehle [8], Garud [9, 10]. For a comprehensive review of several of these models, see Ref. [3]. Mainly for hydrogen action models, see Ref. [11].

The methodology proposed in this paper [12, 13], to build a model which allows an easy representation for modeling, is derived from Ref. [8]: (a) one departed from a two-dimensional diagram which shows the thermodynamic conditions to occur the various modes of stress corrosion in nickel alloys: it is the potential *x* pH or Pourbaix diagram for the material in boiler or primary water at high temperature (300 to 350 °C). It is superimposed with the corrosion submodes, using literature experimental data. Submodes are defined as regions of potential where the different modes of surface material-environment interactions can occur, like stress corrosion, pitting, generalized corrosion or passivation; (b) over this diagram, one adds a third dimension representing a variable, such as initiation time, or crack velocity: the modeling can be done departing from the above referred models adjusted with experimental data.

It also has been applied in Ref. [13] for Alloy 600 specimens in primary water environment at 303 °C, using four different models superimposed over a Pourbaix's potential V-pH marked with corrosion submodes. The modeling has been done using literature data and data from the SSRT (slow strain rating test) equipment installed at CDTN in Brazil [14]. These models can be applied to Brazilian Nuclear Power Plants, and the methodology to mostly of the industries.

2. Description of Three Kinetic Models

These three kinetic models have been chosen to be studied in detail for the case in this paper because it is well accepted to explain intergranular stress corrosion cracking in high temperature water of nickel alloys and stainless steel.

2.1 The Slip-Step Dissolution and Film Rupture Model

This model is one of the most accepted engineering models, developed by General Electric [6]. By this model, crack occurs due metallic corrosion preferentially along an active path as a grain boundary or crystal sleep plane, in an interactive process including electrochemical dissolution and the weakening, rupture and repassivation of the metallic oxide film. The crack growth rate is postulated to be sustained by periodic strain-induced rupture of the film, and the required rupture strain provided by transient creep.

An applied example is showed in Ref. [3] through Eq. (1), for stress corrosion crack growth in 304 stainless steel and nickel base alloys for BWR (boiler water reactors), considering strain rate dependence of the stress intensity.

$$V_{scc} = (7.8\times10^{-3} n^{3.6})(4.1\times10^{-14} K^4)^n \qquad (1)$$

where V_{scc} is the crack growth rate in cm/s, n is an

environment and material chemistry parameter related to repassivation rate, and K is the stress intensity in MPa/m.

This model has been applied to stainless steel and nickel alloys in light water reactors and other structural materials from nuclear plants, including supervisory systems for component life prediction and evaluation *in situ* of machines [3] and is largely accepted as a renowned model.

Ref. [3] presented a validation of experimental data according to the model for Alloy 600, showed in Fig. 2: to lower values of n correspond to the increase of environmental effect, and a decrease of the threshold stress intensity value, above which stress corrosion crack initiates.

Despite of the importance of this model to explain and to quantify stress corrosion cracking in these materials, there are remarks about its scope: Hua and Rebak [16] mentioned that this model was questionable to explain some cases of stress corrosion cracking like the PWR-high temperature water of Alloy 600. For this, this mechanism is not supported by experimental observations, like the independence of the chromium depletion effect over intergranular cracking, and other; notwithstanding researchers from KAPL [17, 18], and others [19], seemed to have a good acceptance of this model for explain this case; so, this is a controversial point, probably derived from the not-well-understood mechanism, which should be better investigated.

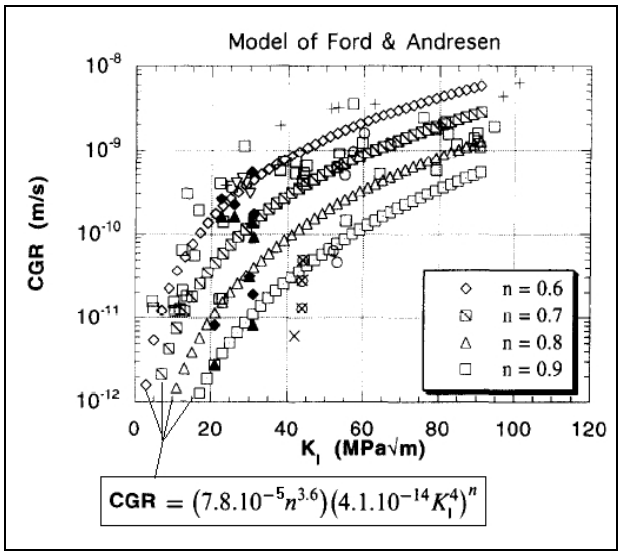

Fig. 2 Crack growth rate (CGR) vs. stress intensity (K_I) predicted by the model of Ford and Andresen, and some experimental data [3].

2.2 The Rice's Creep Model

The crack opening model constrained by creep action proposed in reference [5] tries to quantify the role of the creep in the intergranular stress corrosion cracking process in stainless steels and nickel alloys.

The postulated mechanism of the creep action is constructed over two hypotheses: (a) All grain boundaries perpendicular to the tensile stress direction are evenly separated; (b) The crack opening rate is limited by the neighboring grains which deform according to the creep law.

Fig. 3 shows the mechanism of the creep action: (a) a cavitated grain boundary, subjected to stress σ and separating at rate $\mathrm{d}\delta/\mathrm{d}t$ due to diffusional flow of matter from the cavity surfaces into the grain boundary; (b) axisymmetric geometry employed for analysis of cavity growth: f is the area fraction of cavitated boundary; (c) an isolated, cavitated grain boundary facet in a polycrystal; the stress σ will generally be reduced from the stress σ_∞ which would act across the facet in the absence of cavitation [5].

The average grain boundary separation rate and consequently the average crack opening of a grain facet can be calculated from this model using Eq. (2).

$$\delta_{cal} = \alpha[(\sigma_\infty - \sigma)/\sigma_\infty] \times \varepsilon_{avg} \times d \qquad (2)$$

where δ_{cal} is the calculated average crack opening, α is a dimensionless factor, σ_∞ is the remotely applied uniaxial stress, σ is the tensile stress on cavitated grain boundary, ε_{avg} is the average creep strain, d is the average grain diameter.

This model has been applied to commercial and laboratory Alloy 600 specimens, and compared to the experimental data from constant load tests in order to assess the role of creep in intergranular stress corrosion cracking, showing reasonable modeling results [19].

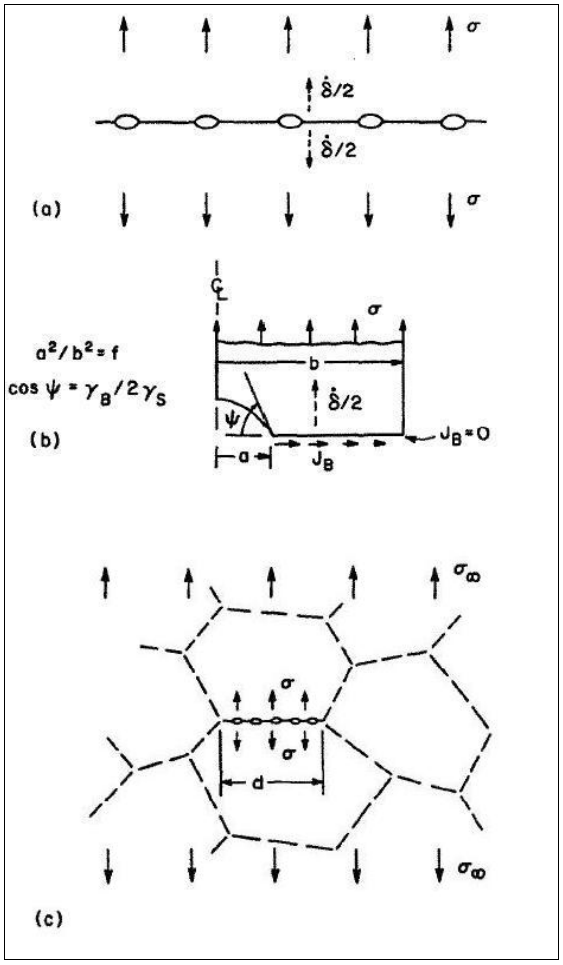

Fig. 3 Sketch of the Rice's creep model mechanism showing: (a) a cavitated stressed grain boundary; (b) geometry employed for analysis of cavity growth; (c) a facet in a polycrystal [5].

2.3 The Creep Model Derived from Monkman-Grant Correlation

This model is based on Rice's considerations about his own [5], whose results were consistent with the diffusional mechanism, in which the rupture time t_r, follows a Monkman-Grant correlation: t_r is proportional to $1/\dot{\varepsilon}_\infty$, where $\dot{\varepsilon}_\infty = d\varepsilon_\infty/dt$ is the creep rate of a similarly loaded polycrystal with uncavitated boundaries.

Thus, the Monkman-Grant correlation can be derived to a model which considers directly the creep strain rate ($d\varepsilon_{CRP}/dt$) on test, as formulated in Eq. (3), where c is a constant.

$$t_r \times \left(d\varepsilon_{CRP} / dt \right) = c \tag{3}$$

3. Example of the Proposed Methodology Application

A methodology used is derived from Ref. [8]: its base (Fig. 4a) is the potential vs. pH or Pourbaix diagram for this material in primary water at high temperature (300 °C to 350 °C) marked with the corrosion submodes. These are determined and superimposed over the Pourbaix diagram, using literature experimental data. The submodes are surface (potential, pH) regions where the different modes of the material-environment interactions can occur, such as stress corrosion, pitting, generalised corrosion or passivation; the three-dimensional diagram (Fig. 4b) shows the thermodynamic conditions where the modes of stress corrosion can occur, applied to Alloy 600. Its third dimension is the "useful strength fraction" of the material as affected by the environment (associated with the stress corrosion susceptibility semi-quantitatively evaluated in SSRT (slow strain rate tests)).

This third dimension variable can be replaced by another one, such as time to initiation, or crack velocity, instead of the stress corrosion cracking strength fraction: this is the fundament of the methodology used here [12, 13].

The experimental work was developed in the CDTN (Nuclear Technology Development Center), located in Belo Horizonte-MG-Brazil; the tests have been done in slow strain rate test machines installed in this center [14].

It was utilized not pre-cracked Alloy 600 MA specimens (Fig. 5), according to the composition and mechanic properties described in Table 1. The standard utilized for SSRT, a dynamic test which is imposed to the specimen a slow strain rate through external force over a monitored section, was ASTM G-129-00. It was realized three tests with applied strain rate $\dot{\varepsilon}_{SSRT} = 3 \times 10^{-7}\ s^{-1}$, test velocity v_T = 33 μm/h, one of these tests in neutral environment (N_2).

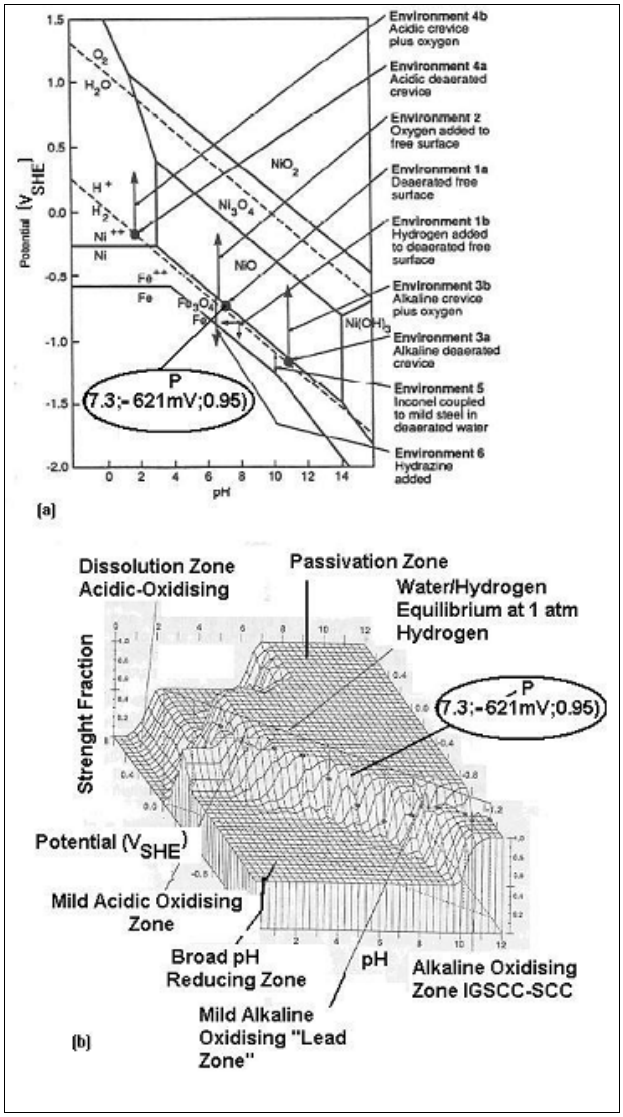

Fig. 4 (a) Bidimensional diagram base, the Pourbaix pH × potential V_{SHE}; (b) Tridimensional diagram: PWSCC strength fraction × pH × potential V_{SHE} with plotted point obtained on CDTN tests: SF (strength fraction) ≈ 0.95; V = – 621 mV; pH = 7.3 [8, 13].

Some resulting microfractographies are showed in Fig. 6. Figs. 7 and 8 show respectively the stress-strain curve, and stress-time of the three tests, one in neutral, and two in primary water environment. From these figures, it can be obtained the parameters of semi-quantitative evaluation to primary water stress corrosion cracking, according to Table 2 [15].

Based on values of this table, we evaluated the strength fraction SF, plotted on Fig. 4b as ≈ 0.95. With

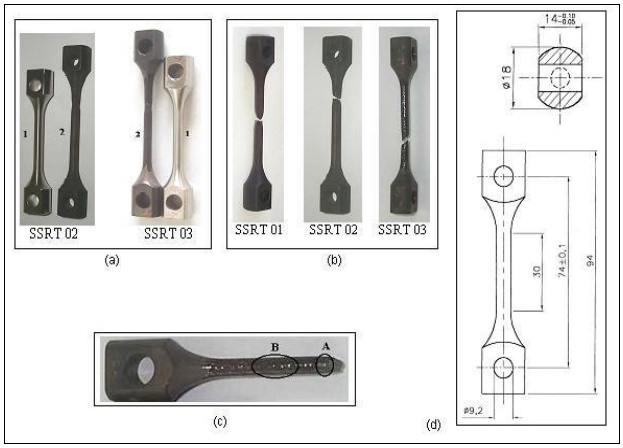

Fig. 5 SSRT results showing Inconel 600MA specimens: (a) SSRT 02 and 03 (PWR environment at 303 ºC and 10 bar), 1-as received, 2-tested; (b) SSRT 01 (neutral environment N_2), strain rate 3.0 × 10^{-7} s^{-1}, ruptured on test; (c) SEM references for microfractographies; (d) specimen geometry on SSRT measured in mm [15].

Table 1 Chemical composition (%), main mechanical properties at 22 ºC and primary water environment conditions of tests of material specimens [15].

Ni	Cr	Fe	Mn	C	Si	S	P
75.05	15.61	8.81	0.22	0.042	0.18	0.0002	0.008
Co	Cu	Al	Ti	Nb	σ_Y (MPa)	σ_R (MPa)	
0.10	0.03	0.08	0.20	0.20	302	632	

Environment of primary water (PW): pressure = 10 MPa, temperature T = 303 °C, 1,200 ppm H_3BO_3, 2.2 ppm LiOH, 35 cm^3 H_2/kg H_2O, 5 ppb O_2

pH and specimen potential estimated at environment temperature, one has obtained the point marked on Figs. 4a and 4b [13].

After the location of the (potential, pH, SF) point representing the thermodynamic conditions of the studied case of stress corrosion cracking to initiate and to grow, we can use a kinetic model as described in Section 2, to be superimposed over it.

The applicable creep model derived from Monkman-Grant correlation, can be deduced immediately based on the results of the CDTN slow strain rate tests. Thus, using Eq. (3), for an average time to initiation of 488.4 h (based on the two tests shown

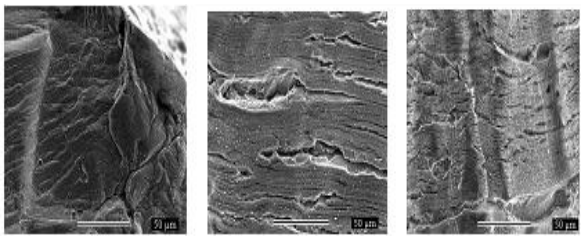

(a) (b) (c)

Fig. 6 SEM-microfractographies, increased 500 times, showing the Alloy 600 MA specimen's lateral surfaces. The tests were realized with slow rate test (3.0×10^{-7} s^{-1}), at 303 ºC and 10 MPa: (a) SSRT 01 (N_2-environment); (b) SSRT 02 (PW-environment); (c) SSRT 03 (PW-environment) [15].

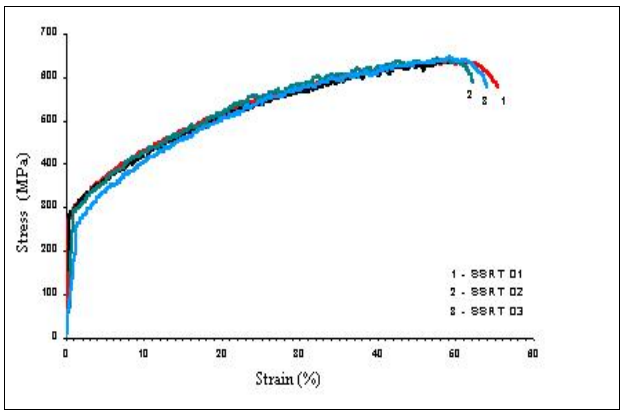

Fig. 7 Alloy 600 MA specimens stress-strain curves. SSRT 01 (neutral environment of N_2), SSRT 02 and 03 (PW environment at 303 ºC and 10 MPa). Initial strain rate of 3.0×10^{-7} s^{-1} [15].

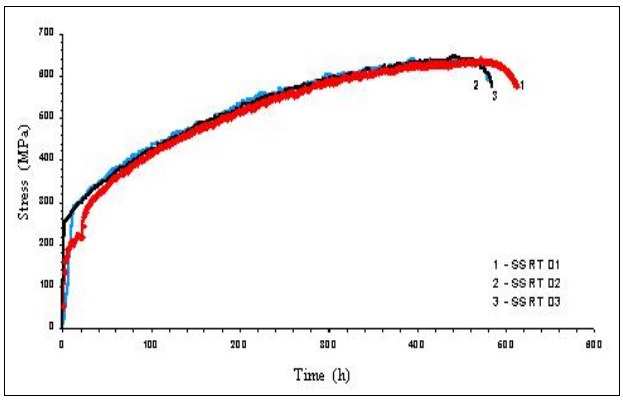

Fig. 8 Alloy 600 MA specimens stress-time curves. SSRT 01 (neutral environment of N_2), SSRT 02 and 03 (PW environment at 303 ºC and 10 MPa). Initial strain rate of 3.0×10^{-7} s^{-1} [15].

Table 2 Parameters of semi-quantitative evaluation to PWSCC according to the tests in CDTN [15].

	Test SSRT No. 1	Test SSRT No. 2
Failure time rate (test environment/neutral environment)	0.94	0.97
Strain rate (test environment/neutral environment)	0.96	0.97
Reduction of area rate (test environment/neutral environment)	0.92	0.92
Time to initiation-estimated (h)	482.4	494.4

in Table 2), and with the average creep strain rate assumed as 2.24×10^{-9} s^{-1} for these Alloy 600 conditions based on evaluation of Ref. [19], one obtains the constant value as 488.4 h × 3600 s × 2.24×10^{-9} $s^{-1} = 0.394 \times 10^{-2}$.

The time to initiation of CDTN tests specimens is represented by Eq. (4).

$$t_i = 0.394 \times 10^{-2} / (\mathrm{d}\varepsilon_{CRP}/\mathrm{d}t) \quad (4)$$

with: t_i = time-to-initiation in h, and $\mathrm{d}\varepsilon_{CRP}/\mathrm{d}t$ = creep rate in s^{-1}.

4. Discussion

The used methodology allowed to represent a third-dimension model considering the stress corrosion cracking thermodynamic propensity to a nickel alloy or a stainless steel in high temperature light water nuclear reactor, to initiate and to propagate.

The base Pourbaix diagram marked with submodes extracted from experiments and literature allows to identify differents corrosion regions, including different submodes of stress corrosion cracking (acidic, alkaline/caustic, with different dissolved oxygen or desaerated/hydrogenated environmental composition); thus, this procedure allows to identify different cases of stress corrosion cracking, which can also have different cracking mechanisms, and consequently shall

be present different models. For example, for Alloy 600 in light water environment, it was presented on Section 2, the description of three of the best probable models: a) there is controversy in application of the slip-step dissolution and film rupture model, instead of creep models; b) there are other models, like some cited on Introduction, which can be fairly adjusted to experimental and/or field data.

The third dimension of the model obtained by this methodology, as originally conceived by Staehle [8], is the "stress corrosion strength fraction", a semi-quantitative parameter extracted from SSRT experimental work. But it can be replaced, by other such as time-to-initiation (as exemplified in this paper), time to propagation, crack velocity, and so on.

The kinetic model used as example is the Monkman-Grant correlation, which considers only the creep contribution in this stress corrosion cracking [5]. It's a very simple relationship with the strain rate applied on test, but it seems also limited on its validity, because the creep strain rate is very difficult to obtain experimentally, and the data are based on literature values.

More elaborated models considering the creep effects are: the Rice creep model (Section 2.2) [5]; the models developed specifically for SSRT from a French group of researchers [20].

We have done the modeling of the same data used in this paper, considering the model of Boursier, and other models [13].

The model of Boursier applied to these data resulted in Eq. (5).

$$t_i = 8.28\times10^{-4}(\mathrm{d}\varepsilon_{SSRT}/\mathrm{d}t)^{-0.67} \quad (5)$$

with t_i = time-to-initiation in day, and $\dot{\varepsilon}_{SSRT} = \mathrm{d}\varepsilon_{SSRT}/\mathrm{d}t$ = strain rate test in s^{-1}.

Comparing Eq. (5) with Eq. (4), it can be observed that in the Boursier's model, the strain rate is affected with an exponent 0.67 < 1 (the creep rate exponent of the Monkman-Grant correlation): we are waiting the opportunity to compare these models' characteristics.

Ref. [20] furnishes a diagram which allows to compare the SSRT results obtained in CDTN with results obtained by the French group. In Fig. 9, this diagram is reproduced with the CDTN's results marked.

Concerning the CDTN's results, we can observe yet that the stress corrosion cracking results are in very good agreement with the obtained by a KAPL research group [17]. If one observes Fig. 6b, it can be estimated a stress corrosion crack length about 100 μm, developed in an average time of 488.4 h; thus based on this, if we consider the 100 μm-flaw as already propagating instead of an initiation-flaw (if Fig. 9 is checked, it can be seen that the CDTN specimens are already in crack growth rate mode), the cracking average propagation velocity results in 5.69 × 10^{-9} cm/s. This CDTN's estimated value is marked over the KAPL's results in Fig. 10, showing a very good agreement.

Both Figs. 9 and 10 show that the CDTN results of experimental work are in very good agreement with both, French and American research groups, concerning experimental work in primary water stress corrosion cracking of Alloy 600.

It can be desirable that CDTN can develop the constant load tests with the nickel alloys specimens, and thus be compared with SSRT work, as done by the French group in Fig. 9 [20]. It can be noted yet that the point marked with CDTN data over Fig. 4 diagrams, is very near the region of equilibrium line Ni/NiO, as expected with Ref. [8]: this region is preferential for stress corrosion cracking susceptibility, also the region of the passive oxide film rupture. The CDTN experimental work can also follow the film-rupture/oxidation mechanism and then its correlate model, as a function of the assumed crack tip strain rate, as showed in Fig. 10 [17].

We strongly encourage other research groups from universities, petrochemical and energy industries, engineering and consulting companies, and other interested in stress corrosion cracking, to use the provided overview and capabilities of the presented methodology in stress corrosion research.

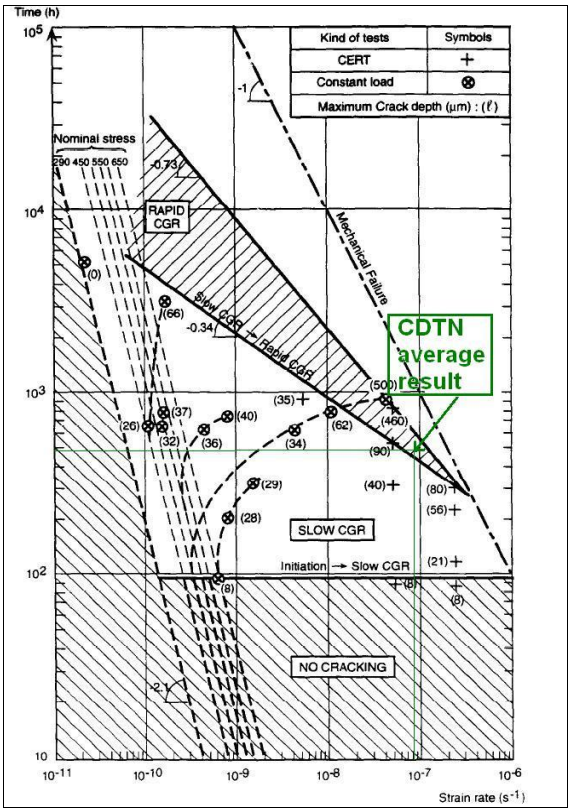

Fig. 9 Fields of cracking for SSRT and constant-load tests as a function of time and strain rate (Alloy 600, tube 6.242R in the as-received condition, primary water at 360 ^{o}C, H_2: 700-800 ml/kg). Marked in green the average result obtained by CDTN [20].

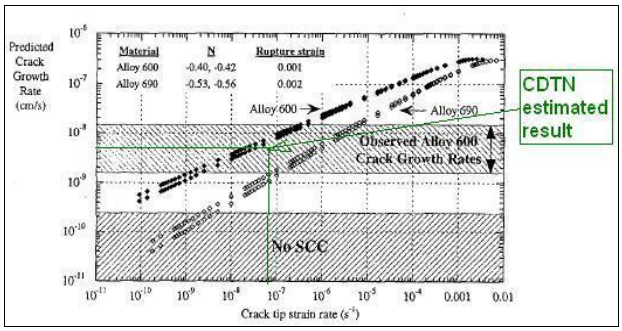

Fig. 10 Predicted crack growth rate for Alloy 600 and Alloy 690 at 338^{o}C, based on the film-rupture/oxidation mechanism, as a function of the assumed crack tip strain rate. Marked in green the estimated result obtained by CDTN [17].

Finally, practically all alloys are susceptible to stress corrosion depending of the existing environment. In the ASM Metal's Handbook [21], one gives a generalized table of material susceptibilities due specific environments. The stress corrosion cracking prediction is a safety, reliability, and design issue in mostly of the engineering structures. As an example, this kind of failure, combined with corrosion-fatigue, caused "the catastrophic collapse of the Silver Bridge in December 1967, when an eyebar suspension bridge across the Ohio River at Point Pleasant, West Virginia, suddenly failed. The main chain joint failed and the whole structure fell into the river, killing 46 people in vehicles on the bridge at the time. Rust in the eyebar joint had caused a stress corrosion crack, which went critical as a result of high bridge loading and low temperature. The failure was exacerbated by a high level of residual stress in the eyebar": This eyebar was made from structural carbon steel [22].

5. Conclusions and Recommendations

It was presented a modeling methodology applied to nickel alloy stress corrosion cracking in high temperature light water reactor, with an example based on slow strain rate test experimental work. This experimental work developed at CDTN-Brazil presented a very good agreement with a French and an American research groups dedicated to this kind of study. Concerning the kinetic models, it was presented three of the most important for the studied case. One of them was applied as an example. All these models suffer controversies in their application, and there is necessity to improve them theoretically and be more experimentally validated: it is highly recommendable to realize more slow strain rate and constant load tests. It was also strongly recommended the use of this methodology and more research investments of industry in this very important safety and reliability engineering issue.

Acknowledgments

Thanks go to CAPES (Coordenação de Aperfeiçoamento de Pessoal de Nível Superior, Brazil) for the research fund, IPEN/CNEN-USP (Instituto de

Pesquisas Energéticas e Nucleares/Conselho Nacional de Energia Nuclear-São Paulo University, Brazil) for the research opportunity and infrastructure, and CDTN/CNEN-UFMG (Centro do Desenvolvimento da Tecnologia Nuclear/Conselho Nacional de Energia Nuclear-Federal University of Minas Gerais, Brazil) for the experimental data availability.

This paper was first electronically published on the ABCM-Brazilian Association of Mechanical Sciences: Proceedings of 21st International Congress of Mechanical Engineering (COBEM 2011), October 24-28, 2011, Natal, RN, Brazil, available online at http://www.abcm.org.br/eventos/anais-de-eventos.

References

[1] M.G. Fontana, N.D. Greene, Corrosion Engineering, McGraw-Hill, New York, 1978.

[2] R.W. Hertzberg, Deformation and Fracture Mechanics of Engineering Materials, John Wiley & Sons, New York, 1989.

[3] R.B. Rebak, Z. Szklarska-Smialowska, The mechanism of stress corrosion cracking of alloy 600 in high temperature water, Corros. Sci. 38 (1996) 971-988.

[4] R.W. Staehle, Bases for predicting the earliest penetrations due to SCC for Alloy 600 on the secondary side of PWR steam generators, Argonne National Laboratory, 2001, NUREG/CR-6737, ANL-01/20 RWS 151, Argonne, Illinois, Sept. 2001.

[5] J.R. Rice, Constraints on the diffusive cavitation of isolated grain boundary facets in creeping polycrystals, Acta metall. 29 (1981) 675-681.

[6] P.L. Andresen, F.P. Ford, Life prediction by mechanistic modeling and system monitoring of environmental cracking of iron and nickel alloys in aqueous systems, Mat. Sci. Eng. A 103 (1988) 167-184.

[7] P.M. Scott, M. Le Calvar, Some possible mechanisms of intergranular stress corrosion cracking of alloy 600 in PWR primary water, in: Proc. Sixth International Symposium on Environmental Degradation of Materials in Nuclear Power Systems-Water Reactors, San Diego, Aug. 1-5, 1993, pp. 657-665.

[8] R.W. Staehle, Combining design and corrosion for predicting life, in: R.N. Parkins (Ed.), Life Prediction of Corrodible Structures, Vol. 1, NACE International, Houston, 1994, pp. 138-291.

[9] J.A. Gorman, K.D. Stavropoulos, W.S. Zemitis, M.E. Dudley, PWSCC prediction guidelines, EPRI Final Report TR-104030 Project 2812-15, Palo Alto, Calif., 1994.

[10] Y.S. Garud, A Simplified Model for assessment of SCC initiation time in Alloy 600, EPRI Final Report TR-109137, Palo Alto, Calif., 1997.

[11] F. Foct, Stress Corrosion Mechanisms in Monocrystalline and Polycrystalline Alloy 600 on PWR: Hydrogen Effects, Ph.D. Thesis, Grenoble, France, 1999. (in French)

[12] O.F. Aly, A.H.P. Andrade, M. Mattar Neto, M. Szajnbok, H.J. Toth, Modelling of primary water stress corrosion cracking (PWSCC) at control rod drive mechanism (CRDM) nozzles of pressurized water reactors (PWR), in: Proceedings of the Second International Conference on Environment-Induced Cracking of Metals (EICM-2), Banff, Alberta, Canada, Sept. 19-23, 2004, pp. 143-151.

[13] O.F. Aly, Modeling of Primary Water Stress Corrosion Cracking at Control Rod Drive Mechanism Nozzles of Pressurized Water Reactors (in Portuguese), Doctorate Thesis, IPEN/CNEN-USP 2006, São Paulo, http://pelicano.ipen.br/PosG30/TextoCompleto/Omar%20Fernandes%20Aly_D.pdf (accessed: Jan. 20, 2011).

[14] M.M.A.M. Schvartzman, C.F.C. Neves, A. Matias, L.I. Lourenço, Susceptibility evaluation to stress corrosion cracking of the Inconel 600 MA in nuclear reactor environment, in: Proceedings of 60th International ABM Congress, ABM: Belo Horizonte, 2005. (in Portuguese)

[15] A. Matias, M.M.A.M Schvartzman, Development of a methodology for evaluation of susceptibility to stress corrosion cracking in nuclear reactor environment, Proceedings of INAC 2005, Santos, Brazil, Sept. 2005. (in Portuguese)

[16] F.H. Hua, R.B. Rebak, The role of hydrogen and creep in intergranular stress corrosion cracking of Alloy 600 and Alloy 690 PWR primary water environments-a review, in: Proceedings of the Second International Conference on Environment-Induced Cracking of Metals (EICM-2), Banff, Alberta, Canada, Sept. 19-23, 2004, pp. 123-141.

[17] S.A. Attanasio, J.S. Fish, D.S. Morton, P.M. Rosencrans, G.S. Was, Y. Yi, Measurement of the fundamental parameters for the film-rupture/oxidation mechanism, KAPL-P-000215, KAPL Atomic Power Laboratory, Schenectady, NY, 1999.

[18] C.D. Thompson, H.T. Krasodomski, N. Lewis, G.L. Makar, Prediction of pure water stress corrosion cracking (PWSCC) in nickel base alloys using crack growth rate models, KAPL-P-000005, KAPL Atomic Power Laboratory, Schenectady, NY, 1995.

[19] G.S. Was, K. Lian, The role of time-dependent deformation in intergranular crack initiation of Alloy 600 steam generator tubing material, NUREG/GR-0016,

University of Michigan-Department of Nuclear Engineering and Radiological Services: Ann Harbor, MI, 1998.

[20] J-M. Boursier, D. Desjardins, F. Vaillant, The influence of strain-rate on the stress corrosion cracking of Alloy 600 in high temperature primary water, Corros. Sci. 37 (3) (1995) 493-508.

[21] ASM: American Society of Metals, ASM Metals Handbook of Corrosion, in: Stress-Corrosion Cracking, Materials Park, Vol. 13, ASM International, OH, 2002, pp. 828-860.

[22] Stress Corrosion Cracking, http://en.wikipedia.org/wiki/Stress_corrosion_cracking (accessed: Jan. 20, 2011).